

Colorectal Cancer Induces Metabolic Reprogramming in Adipose Derived Mesenchymal Stem Cells by Impairing Mitochondrial Function

Marco Varalda¹, Silvia Cracas¹, Irene Volpe¹, Annamaria Antona¹, Jacopo Venetucci¹, Herald Nikaj³, Giovanni Leo¹, Guido Valente^{1,4}, Paolo Marzullo¹, Sergio Gentili^{1,3,5}, Daniela Capello^{1,2}

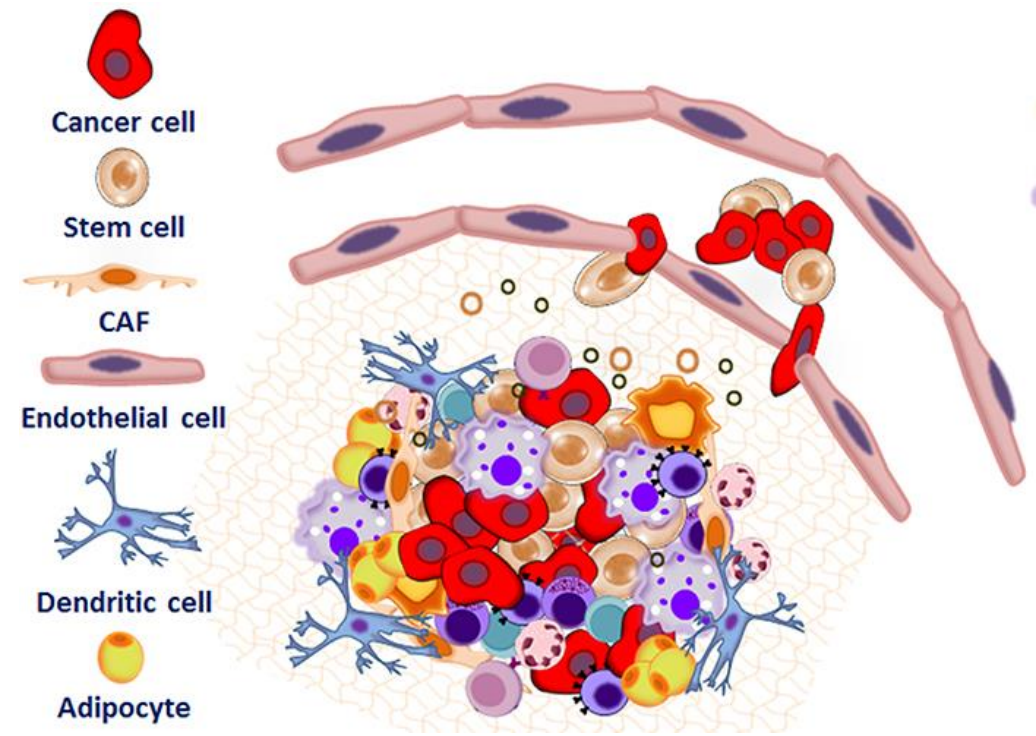
¹Department of Translational Medicine, Centre of Excellence in Aging Sciences, University of Piemonte Orientale, Novara, Italy; ²UPO Biobank, University of Piemonte Orientale, Novara, Italy; ³General Surgery Division, University of Piemonte Orientale, AOU Maggiore della Carità, Novara, Italy; ⁴Pathology Unity, Ospedale "Sant'Andrea", Department of Translational Medicine, University of Piemonte Orientale, Vercelli, Italy; ⁵ Department of Health Sciences University of Piemonte Orientale, Novara, Italy

BACKGROUND

Obesity represents a major risk factor for many pathologies including colorectal cancer (CRC). White adipose tissue (WAT) is mainly involved in the development of these diseases, and adipocytes and MSCs represent important components in tumor microenvironment (TME). Evidence showed that MSCs can differentiate in both cancer associated adipocytes and cancer associated fibroblast (CAF), sustaining tumor progression. Also, cancer can induce tumor-like metabolic reprogramming in MSCs. Conversely, studies report an anti-tumorigenic effect of MSCs.

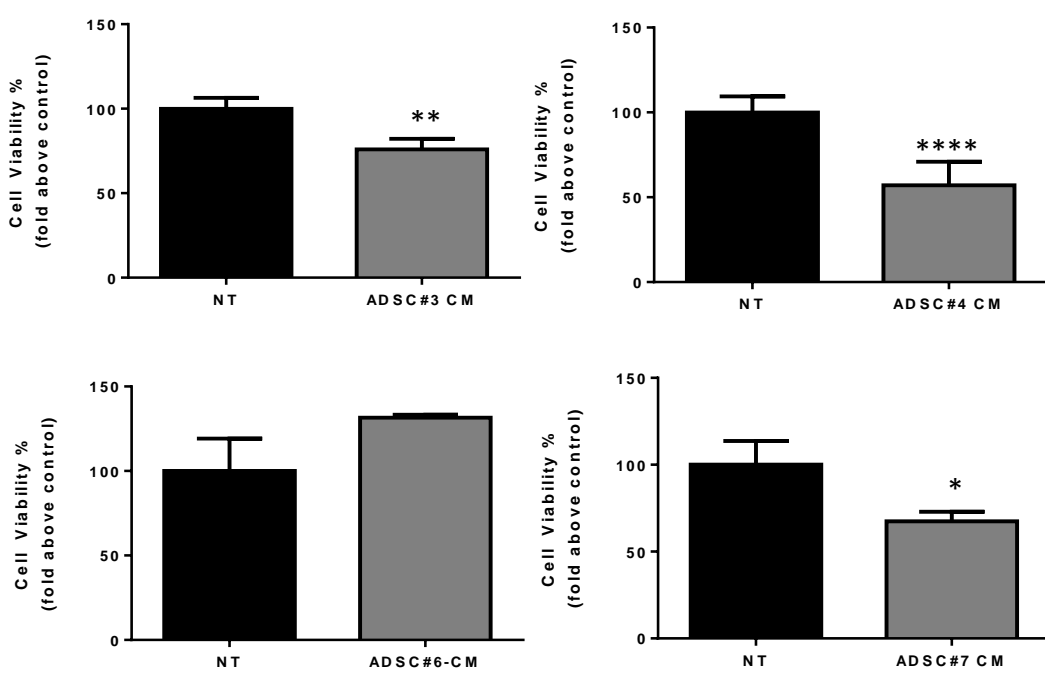
AIM of the STUDY

To investigate the interplay between colorectal cancer (CRC) cells and AT-derived MSCs (ADSCs) to clarify the molecular mechanism behind metabolic reprogramming of ADSCs.



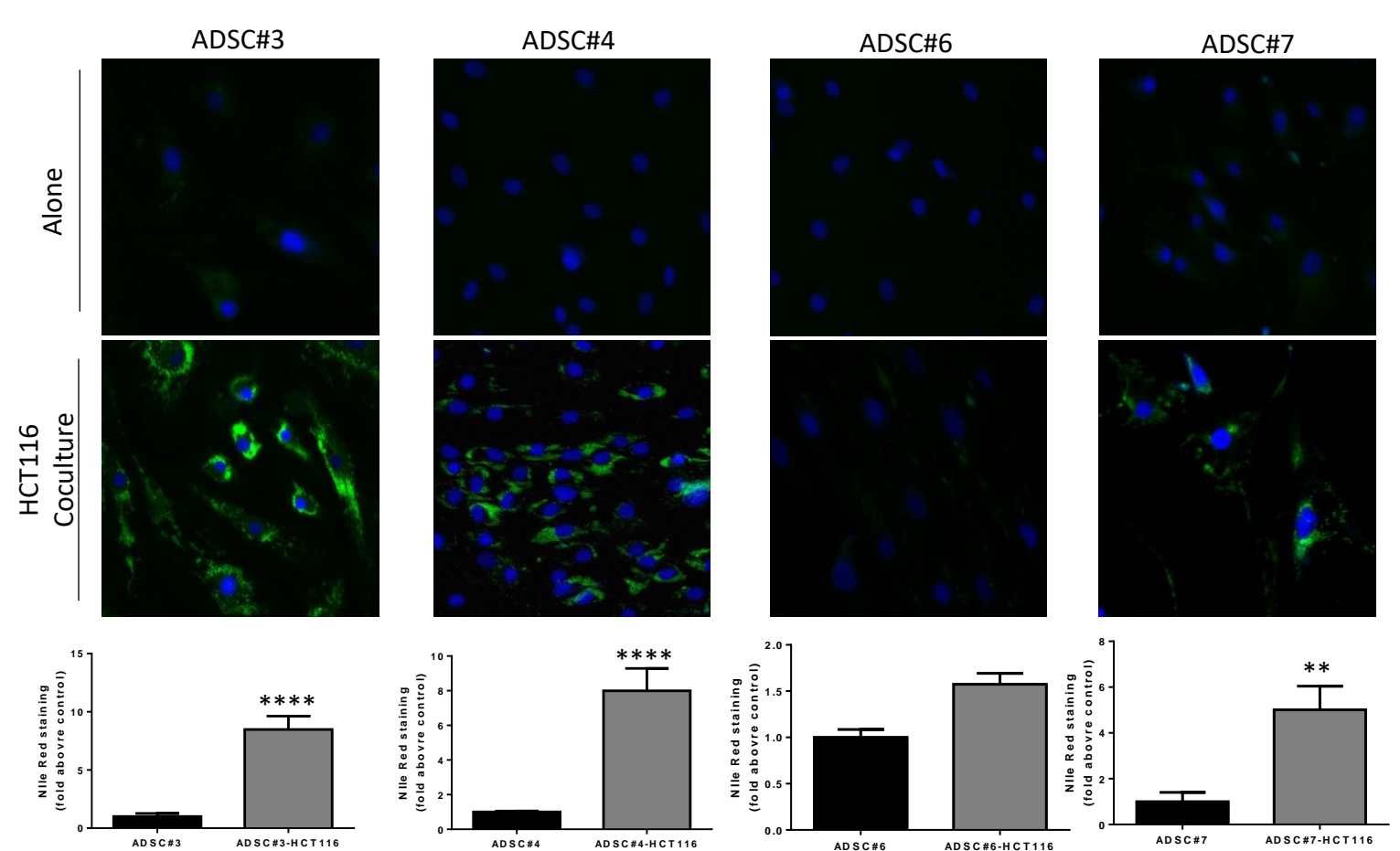
Inzangi et al., 2019

ADSCs conditioned medium treatment reduces CRC cell viability



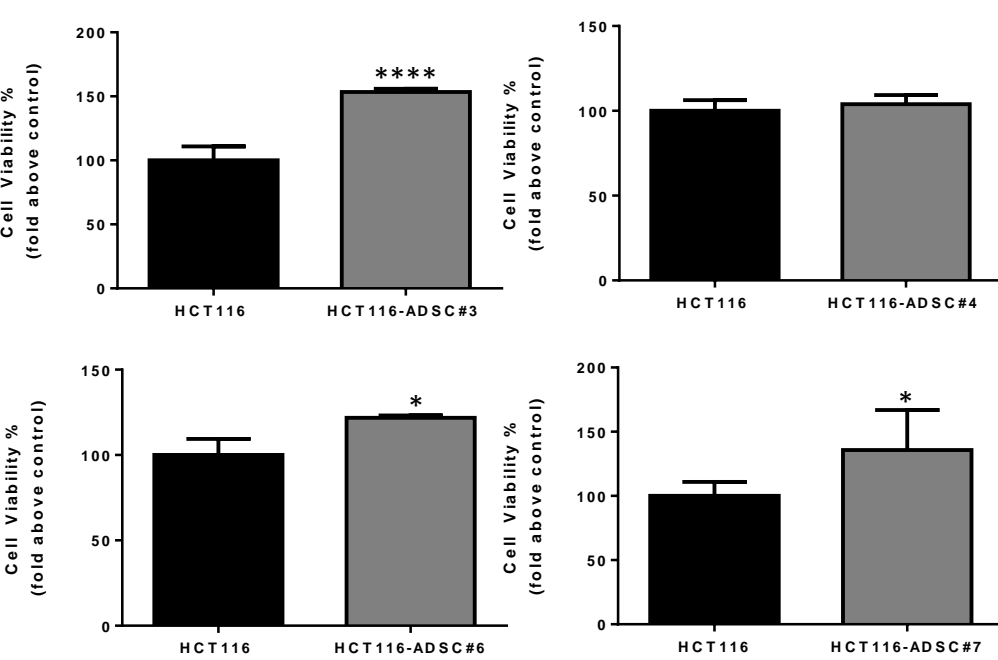
CRC cell line HCT116 was treated for 72h with conditioned medium of four adipose derived mesenchymal stem cell lines (ADSC#3, ADSC#4, ADSC#6, ADSC#7). Viabilities were assessed by CellTox green. **, Student's T-test $p < 0.01$; ***, Student's T-test $p < 0.001$; ****, Student's T-test $p < 0.0001$.

ADSCs cocultured with HCT116 accumulate lipid droplets



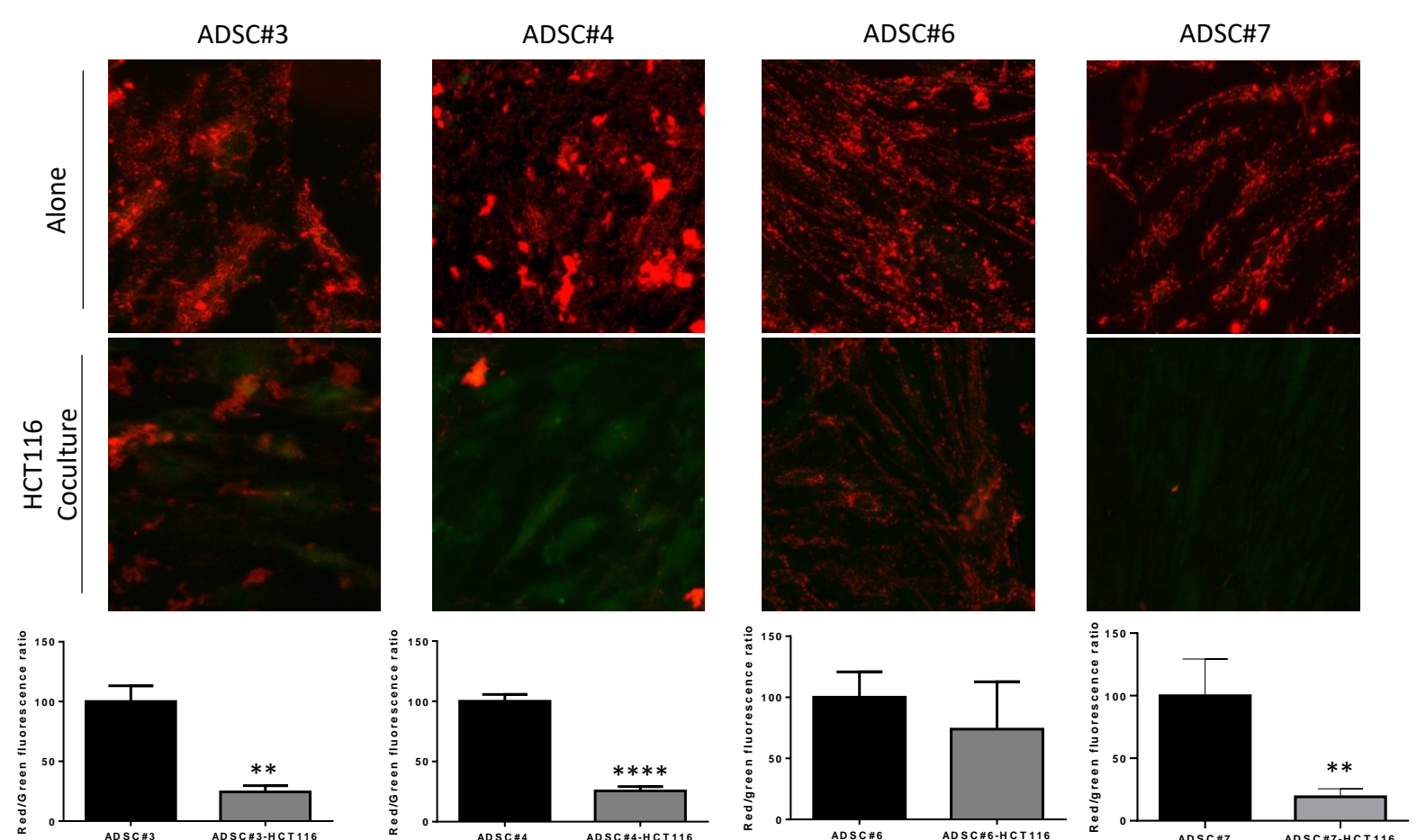
Neutral lipid accumulation was evaluated by Nile red after two weeks coculture of ADSC with HCT116. Representative images of ADSC#3, ADSC#4, ADSC#6 and ADSC#7 alone and in coculture. Histogram showing quantification of red/green fluorescent ratio as fold change relative to control (C). Data are presented as mean \pm standard deviation from two independent experiments, each performed in triplicate. **, Student's T-test $p < 0.01$. ****, Student's T-test $p < 0.0001$.

ADSCs conditioned medium treatment reduces CRC cell viability



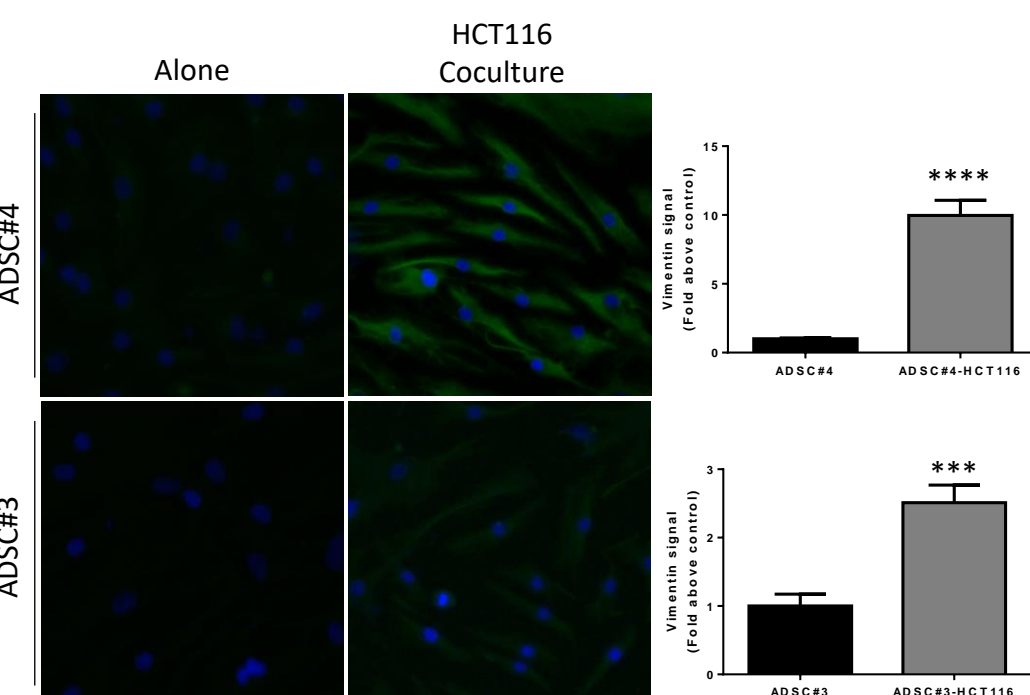
HCT116 viability was evaluated by cell count using trypan blue after 2 weeks coculture with ADSC (ADSC#3, ADSC#4, ADSC#6, ADSC#7). *, Student's T-test $p < 0.05$; **, Student's T-test $p < 0.01$; ****, Student's T-test $p < 0.0001$.

Mitochondrial depolarization of ADSCs cocultured with HCT116



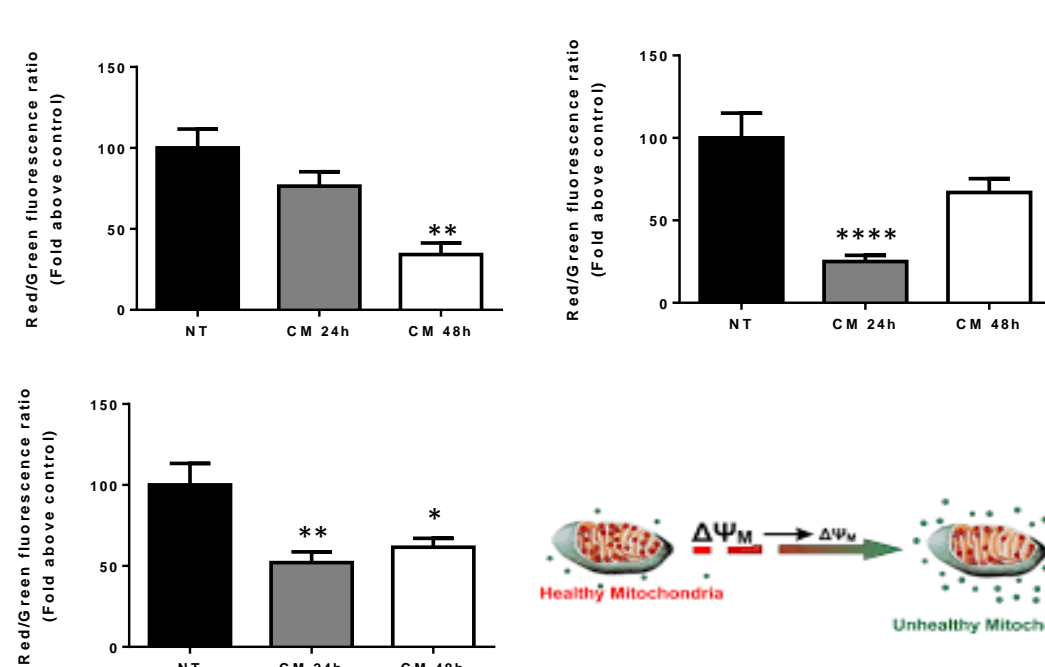
Mitochondrial membrane potential depolarization was evaluated by JC-1 staining after two weeks coculture of ADSC with HCT116 cells. Representative images of ADSC#3, ADSC#4, ADSC#6 and ADSC#7 alone and in coculture. Histogram showing quantification of red/green fluorescent ratio as fold change relative to control (C). Data are presented as mean \pm standard deviation from two independent experiments, each performed in triplicate. **, Student's T-test $p < 0.01$. ****, Student's T-test $p < 0.0001$.

Vimentin expression in ADSCs cocultured with CRC cells



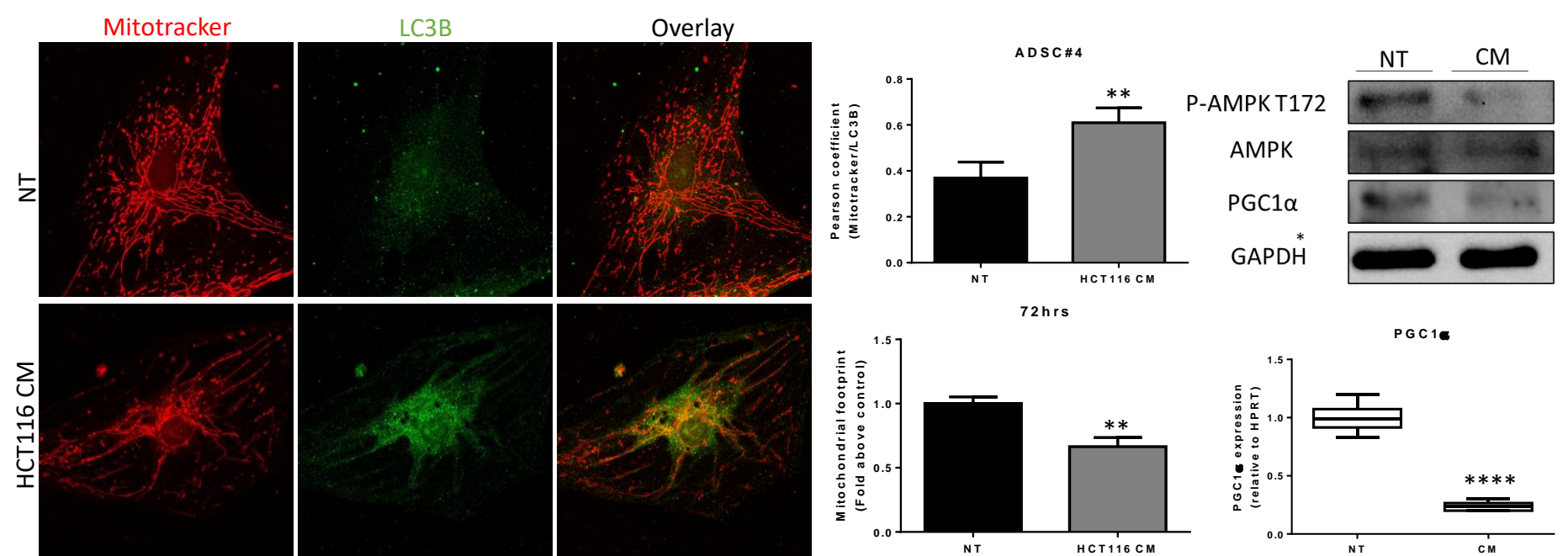
Vimentin expression was evaluated by immunofluorescence after two weeks coculture of ADSC with HCT116. Representative images of ADSC#3 and ADSC#4 alone and in coculture. Histogram showing quantification of green fluorescent signal as fold change relative to control. ***, Student's T-test $p < 0.001$. ****, Student's T-test $p < 0.0001$.

HCT116 conditioned medium treatment induces mitochondrial depolarization



Mitochondrial depolarization was evaluated by JC-1 in ADSC#3, ADSC#4 and ADSC#7 after 24 and 48hrs treatment with HCT116 conditioned medium, normal medium was used as negative control. Histogram showing quantification of red/green fluorescent ratio expressed as fold change relative to control. Data are presented as mean \pm standard deviation from two independent experiments. *, Student's T-test $p < 0.05$; **, Student's T-test $p < 0.01$; ****, Student's T-test $p < 0.0001$.

Mitochondrial footprint reduction in ADSCs is associated with mitophagy and mitochondrial biogenesis inhibition



Mitophagy and mitochondrial footprint were evaluated in ADSC#4 after 72hrs treatment with HCT116 conditioned medium, normal medium was used as negative control. Pictures were acquired by confocal microscope. Mitochondria were stained using Mitotracker Red and LC3B was stained using LC3B primary antibody and Alexafluor 488 secondary antibody (green). Histogram showing quantification of Mitotracker and LC3B co-localization expressed as Pearson coefficient. Histogram showing quantification of mitochondrial footprint expressed as mitochondrial footprint area/total area. Data are presented as mean \pm standard deviation from two independent experiments. **, Student's T-test $p < 0.05$. Western blot showing P-AMPK T172 phosphorylation and PGC1 α expression. Graph showing PGC1 α expression evaluated by real time PCR. Data are expressed as fold change relative to control. ****, Student's T-test $p < 0.0001$.

CONCLUSION

Our results evidence a strong interplay between ADSCs and cancer cells. Whereas naive ADSCs conditioned medium can inhibit cancer cell proliferation, ADSCs co-cultured with cancer cells display metabolic reprogramming by lipid droplets accumulation, mitochondrial depolarization, CAF differentiation and sustain tumor growth. At the same time, ADSCs treated with HCT116 conditioned medium show mitochondrial depolarization, mitochondrial footprint reduction and mitophagy, suggesting a mechanism of metabolic reprogramming. Our data contribute to understand the role of AT in tumor development and progression and will help to identify new druggable pathways and anti-cancer therapeutic strategies.